Environmental Science and Pollution Research (2020) 27:20770–20785
https://doi.org/10.1007/s11356-020-08473-1

RESEARCH ARTICLE

Adsorption of Sudan-IV contained in oily wastewater on lipophilic activated carbons: kinetic and isotherm modelling

Jose L. Diaz de Tuesta[1] · **Adrián M. T. Silva**[2] · **Joaquim L. Faria**[2] · **Helder T. Gomes**[1]

Received: 13 December 2019 / Accepted: 16 March 2020 / Published online: 4 April 2020

Abstract

Up to nine kinetic and fourteen isotherm adsorption models are employed to model the adsorption of Sudan IV, a lipophilic model pollutant present in a biphasic mixture of cyclohexane-water system to simulate oily wastewater. Six different modified activated carbons were used as adsorbents. The highest amount adsorbed of Sudan IV was found in the material prepared by successive treatments of the parent commercial activated carbon Norit ROX 0.8 with nitric acid and urea, followed by thermal treatment at 800 °C under continuous flow of nitrogen. Kinetic and isotherm adsorption models can be employed to simulate the process, since the effect of the presence of water in the adsorption of Sudan IV from the cyclohexane phase was found to be negligible, owing to the high lipophilic character of both adsorbent and adsorbate. All kinetic and isotherm coefficients, coupling with statistical parameters (r^2, adjusted r^2 and sum of squared errors), are determined by non-linear regression fitting and compared to literature data. The model of Avrami is found to be the most appropriate model to represent the adsorption of the pollutant in any of the six modified carbons tested, the highest value of the kinetic constant being 0.055 min^{-1}. The isotherm adsorption is well-modelled by using the general isotherm equation of Tóth and the multilayer Jovanović expression for the adsorption of Sudan-IV on that material, resulting in a high monolayer uptake capacity ($q_m = 193.6$ mg g^{-1}).

Keywords Triphasic adsorption · Lipophilic pollutant · Activated carbon · Modelling · Denitrification · Oil purification

Introduction

Nowadays, oil industry, oil refining, oil storage, transportation and petrochemical industries generate large volume of water containing insoluble liquid organic compounds, resulting in oily wastewater (Abousnina et al. 2014; Al-Futaisi et al. 2007; Chen and He 2003; Machín-Ramírez et al. 2008; Yu et al. 2017). In the production of oil or natural gas, the produced water is the largest by-product and the effluent may reach oil-to-water volume ratio of 1:3 (Abousnina et al. 2014). In refining of crude oil and in the manufacturing of fuels, lubricants and petrochemical intermediates, the oily wastewaters may consist of both oil and grease containing many other toxic organic pollutants (Diya'uddeen et al. 2011). The cleaning of oil products is also a subject of interest in the field of fossil fuels for the removal of compounds containing sulphur or nitrogen elements, which are the main responsible products for acid rain (Oliveira et al. 2014). Within this context, the removal of those undesired compounds from oils is important, not only to mitigate environmental pollution, but also to recover the considered oil product, whose quality is affected by the presence of the pollutants. Selective oxidation of oily wastewater allows removing a lipophilic pollutant from the oily phase, leading to generate hydrophilic oxidized products, which are transfered to the aqueous phase (Diaz de Tuesta et al. 2019).

In a previous work, we have shown the effect of several operating conditions (pH, water/oil ratio, particle size, initial pollutant concentration and the presence of an emulsifier) on the adsorption of Sudan-IV (S-IV), a high-lipophilic model

Responsible editor: Tito Roberto Cadaval Jr

Electronic supplementary material The online version of this article (https://doi.org/10.1007/s11356-020-08473-1) contains supplementary material, which is available to authorized users.

✉ Jose L. Diaz de Tuesta
jl.diazdetuesta@ipb.pt

[1] Centro de Investigação de Montanha (CIMO), Instituto Politécnico de Bragança, Campus de Santa Apolónia, 5300-253 Braganca, Portugal

[2] Laboratory of Separation and Reaction Engineering - Laboratory of Catalysis and Materials (LSRE-LCM), Faculdade de Engenharia, Universidade do Porto, Rua Dr. Roberto Frias, 4200-465 Porto, Portugal

pollutant with toxic hazards properties (Noguerol-Cal et al. 2008; Sun et al. 2015), using modified activated carbons and a biphasic mixture cyclohexane-water in order to simulate contaminated oily wastewater (Diaz de Tuesta et al. 2018). In that study, it was found that the water/oil (W/O) ratio has no effect on the adsorption process, as consequence of the lipophilic character of the pollutant (not detected in the aqueous phase) and the characteristics of the modified activated carbons used (preferentially found in the oil phase). However, more studies should be addressed seeking the complete removal and modelling of the adsorption of S-IV, which is known as a harmful colouring additive widely used in fuels, waxes, plastics and floor and shoe polishes. Kinetic adsorption data allow to describe the dynamics of the adsorption mechanism and to evaluate the time required to remove a specific solute (Kumar and Sivanesan 2006; Savić and Vasić 2006). The modelling of adsorption isotherms is also useful to understand the interaction between the adsorbate (pollutant) and the adsorbent.

In the kinetic and isotherm modelling of the adsorption process in wastewater treatment are found several equations that sometimes are wrongly used, or confused with each other, as discussed along this work. In addition, linear regression is typically used, despite not being recommended (El-Khaiary and Malash 2011; Foo and Hameed 2010; Kumar et al. 2008; Kumar and Sivanesan 2006).

The current work deals with a revision of the kinetic and isotherm modelling of pollutant adsorption from aqueous matrices in the treatment of wastewater and its application in the adsorption of the model pollutant S-IV from a biphasic medium oil-water using lipophilic activated carbons as adsorbents. Temperatures in the range 25–50 °C were studied. Up to nine kinetic models and 14 isotherm models, typically used in the adsorption of pollutants in one-phase aqueous solution, were assessed by non-linear regression.

Materials and methods

Reagents

The activated carbon used as adsorbent in this work was Norit ROX 0.8. S-IV (general purpose grade) and cyclohexane (99.99%) which were obtained from Fisher Chemical, whereas H_2O_2 (30%, w/v) was obtained from Panreac. Sulphuric acid (96–98 wt.%), nitric acid (65 wt.%) and urea (65 wt.%) were obtained from Riedel–de-Haën. Distilled water was used throughout the work.

Modified activated carbons

First, powdered activated carbon (PAC) was obtained by grinding and sieving the commercial activated carbon to a particle range from 106 to 250 μm and then PAC was chemically modified by liquid phase, thermal and hydrothermal treatments, resulting in the production of five additional activated carbon samples, following the procedures reported elsewhere (Diaz de Tuesta et al. 2018; Gomes et al. 2011; Gomes et al. 2010; Ribeiro et al. 2013). Three of the samples were modified directly from PAC by liquid phase treatments with hydrogen peroxide (PACHP), sulphuric acid (PACSA) and HNO_3 (PACNA). The treatment with H_2O_2 of 25 g of PAC was conducted in a round-bottom glass flask containing 500 mL of H_2O_2 30% (w/v) at room temperature for 24 h. In H_2SO_4 treatment, the same amount of PAC was immersed in 500 mL of 18 M acid solution at 150 °C during 3 h and in HNO_3 oxidation, 25 g of PAC was placed in 500 mL of 5 M nitric acid solution at 110 °C for 3 h. Then, all samples were washed with distilled water until the rinsing waters reach neutral pH and further dried in an oven at 110 °C overnight. The last two materials were obtained in successive treatments of the PACNA sample. First, 2 g of PACNA was treated with 50 mL of 1 M urea solution and kept in a 125-mL removable Teflon vessel inserted in a stainless steel body (Parr Instrument co., USA) reactor under autogenous pressure at 200 °C for 2 h. The recovered material was washed and dried as previous samples, resulting in the PACNAU material. Secondly, 1 g of PACNAU was heated, under a nitrogen flow (100 cm^3 min^{-1}) at 120, 400 and 600 °C during 1 h at each temperature and then at 800 °C for 4 h, resulting in the PACNAUT material. An extensive characterization of these activates carbon materials can be found in previous reports (Diaz de Tuesta et al. 2018; Karimi et al. 2018).

Kinetic and equilibrium adsorption studies

Kinetic adsorption experiments were conducted in a 250-mL well-stirred round-bottom glass flask, equipped with a reflux condenser and a temperature measurement thermocouple. First, both cyclohexane and water liquid phases were added using a total volume of 100 mL within the two phases and the water/oil (W/O) ratio of 1:10. Then, this medium was heated to 50 °C by immersion in an oil bath at controlled temperature and 2.5 g L^{-1} of adsorbent was loaded, defining this instant as the initial time of the run ($t_0 = 0$ h). The experiments were conducted during 24 h and were monitored by taking samples periodically from the organic phase to determine the concentration of S-IV (the corresponding quantity of water to keep a ratio of W/O = 1:10 was also withdrawn). The concentration of S-IV in the organic phase was quantified by using UV/Vis spectrophotometry (Jasco V530) at a wavelength of 520 nm.

Equilibrium adsorption experiments were performed to obtain the adsorption equilibrium isotherms of S-IV. In each experiment, 2.5 g L^{-1} of adsorbent was contacted in a flask with a biphasic system composed by 8 mL of organic phase solution containing different initial concentrations of S-IV (30–600 mg L^{-1}) and 0.8 mL of water (W/O = 1:10). The flasks were placed in an orbital shaker, at 50 ± 1 °C, until equilibrium was reached (72 h). Additionally, the activated carbon performing better was analysed at low temperature (25 °C) in order to evaluate the thermodynamic of the adsorption of S-IV on its surface.

Selected kinetic and equilibrium runs were carried out in triplicate, in order to assess reproducibility and error of the experimental results obtained in the adsorption of S-IV from the triphasic system.

Modelling of adsorption kinetic and isotherm equilibrium

Since both pollutant and adsorbent are lipophilic and hence only present in the oil phase, the amount of dye adsorbed by the adsorbent was calculated applying Eq. 1:

$$q_t = \frac{(C_0 - C_t) \cdot V_{OP}}{W} \tag{1}$$

where q_t is the amount of S-IV adsorbed per unit mass of adsorbent at the time t (mg·g^{-1}), C_0 is the initial S-IV concentration in the organic phase (OP) (mg·L$_{OP}^{-1}$), C_t is the S-IV concentration in the OP at the adsorption time t (mg·L$_{OP}^{-1}$), W is the adsorbent mass (g) and V_{OP} is the volume of the organic phase (L$_{OP}$).

Using a non-linear regression, it is possible to achieve better-fitted equations than with a linearized method which minimizes the sum of squared error of the linearized "y" function (Kumar and Sivanesan 2006). Thus, kinetic and equilibrium models were fitted by employing a nonlinear method with successive numerical iteration based on the generalized reduced gradient algorithm (solver tool of Excel) for least error sum of squared (SSE) minimization of q_t, Eq. (2):

$$SSE = \sum_{i=1}^{n} \left(q_{t,exp,i} - q_{t,model,i} \right)^2 \tag{2}$$

where $q_{t,exp,i}$ (mg g^{-1}) represents the amount of S-IV adsorbed per unit mass of adsorbent at time t in the measured adsorption experiments (or equilibrium ones, q_t being expressed as q_e) and $q_{t,model,i}$ (mg g^{-1}) the respective calculated values given by the model.

The models were evaluated by the adjusted determination factor (r^2_{adj}), calculated from determination factor (r^2) as follows (Eqs. 3 and 4):

$$r^2 = \frac{SSR}{SST} = \frac{\sum_{i=1}^{n} \left[\left(q_{t,model,i} - \overline{q_{t,model}} \right)^2 \right]}{\sum_{i=1}^{n} \left[\left(q_{t,model,i} - \overline{q_{t,model}} \right)^2 \right] + \sum_{i=1}^{n} \left[\left(q_{t,exp,i} - q_{t,model,i} \right)^2 \right]} \tag{3}$$

$$r^2_{adj} = 1 - \frac{n-1}{n-k-1} \cdot \left[1 - r^2 \right] \tag{4}$$

where SSR and SST are the residual and total sum of square, n is the total number of values (i) modelled and k is the number of independent variables. r^2_{adj} is used to compare the models taking into account the degrees of freedom or the number of parameters from each model equation (Foo and Hameed 2010).

Results and discussion

Adsorption kinetics

In the S-IV adsorption runs performed with the prepared activated carbon materials, both the pollutant and the carbon adsorbents are found only in the organic phase, as a consequence of the lipophilic character of both adsorbate and adsorbent.

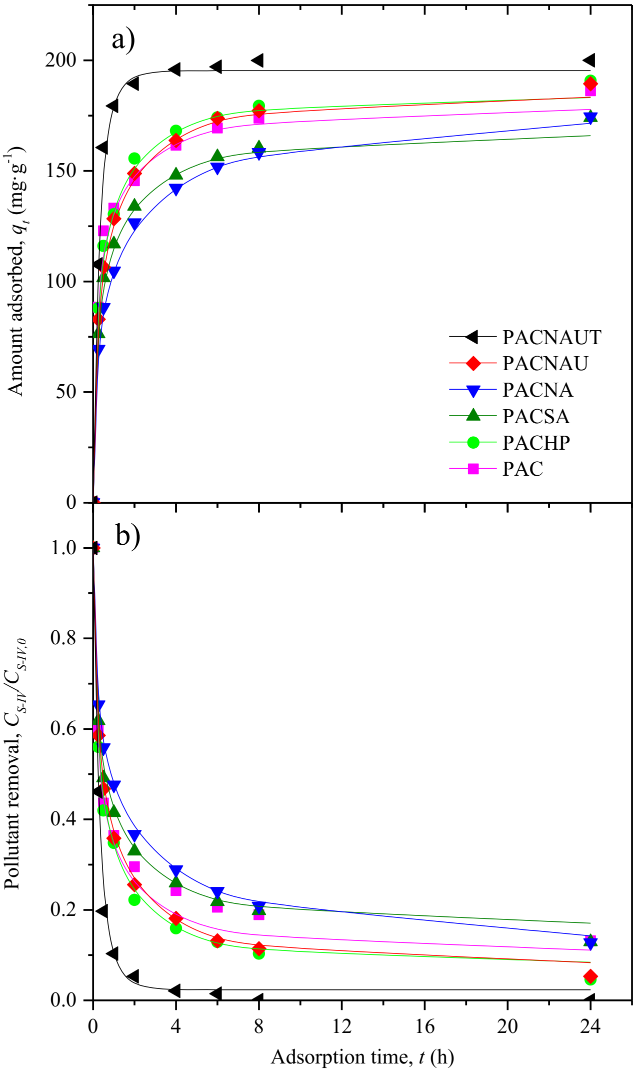

Fig. 1 Effect of the activated carbon modifications in the adsorption of S-IV (experimental values are shown as symbols and the values calculated from the proposed kinetic model are shown as curves). Operating conditions: biphasic mixture W/O = 1:10 of water/cyclohexane, natural pH, 50 °C, $C_{S\text{-}IV,0}$ = 500 mg L^{-1}, $C_{adsorbent}$ = 2.5 g L^{-1} of organic phase

The results obtained are depicted in Fig. 1. As can be observed, the amount of dye adsorbed per unit mass of adsorbent was found to be in the range from 170 to the maximum amount of S-IV adsorbed (200 mg g^{-1}) from the organic liquid phase (total removal) after 24 h with the prepared activated carbons. The complete removal of the pollutant, and hence the complete removal of the N-content and colour from the organic phase, was achieved with the chemically and thermally modified material PACNAUT. The result can be ascribed to its high textural development, as consequence of the modifications made to the powdered commercial carbon, obtaining the highest specific surface and porous volume amongst all tested materials (Table 1). According to Fig. 1, the experimental data show initial stages where quick adsorption occurs and all runs reach the equilibrium state after 8 h under the following operating conditions: biphasic mixture W/O = 1:10 of water/cyclohexane, natural pH, 50 °C, $C_{S\text{-}IV,0} = 500$ mg L^{-1}, $C_{adsorbent} = 2.5$ g L^{-1} of organic phase. Exceptionally, the adsorption of S-IV with PACNAUT almost reaches the equilibrium after 4 h. At this time, 98% of S-IV is removed from the organic phase (complete adsorption of S-IV occurs after 8 h).

The adsorption of S-IV onto the unmodified (PAC) and onto all the modified (PACSA, PACHP, PACNA, PACNAU and PACNAUT) activated carbon adsorbents was evaluated implementing nine kinetic models that are typically applied in wastewater treatment by adsorption in aqueous phase solutions (exempted from oil), namely pseudo-first-order (Lagergren 1898), pseudo-second-order (Ho and McKay 1999), Bangham (Bangham and Burt 1924), Elovich (Low 1960), Avrami (Avrami 1939; Avrami 1940), Dünwald-Wagner (Dünwald and Wagner 1934), Weber-Morris (Weber and Morris 1963), Boyd-Reichenberg model (Boyd et al. 1947; Reichenberg 1953) and double-exponential model (DEM). All kinetic equations are summarized in Table 2, as amount of dye adsorbed per unit mass of adsorbent (q_t) as function of contact time (t), as well as the constant parameters involved.

The pseudo-first-order model was the first equation describing the adsorption rate based on the monolayer adsorption capacity (Gurses et al. 2006). The pseudo-second-order model (Al-Ghouti et al. 2009; Malash and El-Khaiary 2010a) describes an adsorption process controlled by chemisorption, involving valence forces through sharing or exchange of electrons between the solvent and the adsorbate. In some studies, a kinetic equation with a call-name hyperbolic model can be found (Cotoruelo et al. 2009a; Cotoruelo et al. 2009b; García-Mateos et al. 2015), as expressed by Eq. 5:

$$q_t = \frac{k_h \cdot q_h \cdot t}{1 + k_h \cdot t} \tag{5}$$

where k_h is an empirical constant and q_h represents the asymptotic q_t value at given experimental conditions, that is, the amount adsorbed at equilibrium stage. However, the hyperbolic model is nothing other than a transformation of the second-order kinetic model, as given by Eq. 6:

$$q_t = \frac{1}{\frac{1}{(k_s \cdot q_e{}^2) \cdot t} + \frac{1}{q_e}} \cdot \frac{(k_s \cdot q_e{}^2) \cdot t}{(k_s \cdot q_e{}^2) \cdot t} = \frac{k_s \cdot q_e{}^2 \cdot t}{1 + k_s \cdot q_e \cdot t} \tag{6}$$

Thus, the constant parameter of the hyperbolic model (k_h) is equivalent to the multiplication of the pseudo-second-order constant by the equilibrium adsorption capacity ($k_h = k_s \cdot q_e$). Both parameters are constants at given operating conditions.

A pore diffusion model of Bangham is also evaluated, as well as the chemical adsorption from the Elovich equation, expressed as Eq. 7 (Doğan et al. 2007; Rodriguez et al. 2009):

$$\frac{dq_t}{dt} = \alpha \cdot \exp(-\beta \cdot q_t) \tag{7}$$

Typically, in published reports (Ho 2006; Qiu et al. 2009; Rodriguez et al. 2009), it is used a simplified form (Eq. 8) from the integration of Eq. 7, given by Chien and Clayton (Chien and Clayton 1980):

$$q_t = \frac{1}{\beta} \cdot \ln(\alpha \cdot \beta) + \frac{1}{\beta} \cdot \ln(t) \tag{8}$$

Equation 8 has been largely used, but it is a modification of the integration of Eq. 7, assuming $\alpha \cdot \beta \cdot t >> 1$ with the purpose to linearize the Elovich equation (Chien and Clayton 1980). For this reason, in this work, the integrated form of Elovich

Table 1 Textural properties of the powdered activated carbons determined from BET and *t*-plot methods (Diaz de Tuesta et al. 2018)

	S_{BET} (m^2 g^{-1})	S_{ext} (m^2 g^{-1})	S_{mic} (m^2 g^{-1})	V_{mic} (mm^3 g^{-1})	V_{mic}/V_{Total} (%)	W_{mic} (nm)
PAC	885 ± 10	160 ± 2	725 ± 12	314 ± 1	58	1.73 ± 0.03
PACSA	862 ± 9	150 ± 2	712 ± 11	308 ± 1	59	1.72 ± 0.03
PACHP	893 ± 10	159 ± 2	734 ± 12	319 ± 1	58	1.73 ± 0.03
PACNA	889 ± 10	170 ± 2	719 ± 12	311 ± 1	57	1.72 ± 0.03
PACNAU	960 ± 11	181 ± 2	778 ± 12	336 ± 1	58	1.72 ± 0.03
PACNAUT	1055 ± 11	197 ± 2	858 ± 12	367 ± 1	58	1.71 ± 0.03

Table 2 Kinetic adsorption models

Kinetic model	Non-linear equation	Parameter
Pseudo-first-order (Lagergren equation)	$q_t = q_e \cdot (1 - \exp(-k_f \cdot t))$	q_e, k_f
Pseudo-second-order (Ho and McKay equation)	$q_t = \frac{1}{\frac{1}{(k_s \cdot {q_e}^2)} \cdot \frac{1}{t} + \frac{1}{(q_e)}}$	q_e, k_s
Bangham	$q_t = k_r \cdot t^{1/m}$	k_r, m
Elovich	$q_t = \frac{1}{\beta} \cdot \ln(\alpha \cdot \beta \cdot t + 1)$	α, β
Avrami	$q_t = q_e(1 - \exp(-k_{AV} \cdot t)^{n_{AV}})$	q_e, k_{AV}, n
Dünwald-Wagner intraparticle diffusion	$q_t = q_e \cdot \sqrt{1 - \exp(-k_{DW} \cdot t)}$	q_e, k_{DW}
Boyd-Reichenberg model	For $q_t/q_e < 0.85$, $q_t = q_e \cdot \frac{3}{\pi} \cdot \left[1 - \left(1 - \frac{(B \cdot t)^2}{\sqrt{\pi}}\right)^2\right]$ For $q_t/q_e > 0.85$, $q_t = q_e \cdot \left(1 - \frac{6}{\pi^2} \cdot \exp(-B \cdot t)\right)$ $D_i = B \cdot \left(\frac{r}{\pi}\right)^2$	q_e, B
Weber-Morris intraparticle diffusion	$q_t = k_{id} \cdot \sqrt{t} + C$	k_{id}, C
Double-exponential model (DEM)	$q_t = q_e - \frac{D_1}{m_a} \cdot \exp(-K_1 \cdot t)$ $-\frac{D_2}{m_a} \cdot \exp(-K_2 \cdot t)$ $K_1 >>> K_2$: $q_t = q_e - \frac{D_2}{m_a} \cdot \exp(-K_2 \cdot t)$	q_e, $\frac{D_2}{m_a}$, K_2

equation (Eq. 9) was used by applying the boundary conditions $q_t = 0$ at $t = 0$ and $q_t = q_t$ at $t = t$, without the aged assumption realized by Chien and Clayton:

$$q_t = \frac{1}{\beta} \cdot \ln(\alpha \cdot \beta \cdot t + 1) \tag{9}$$

The Avrami kinetic equation determines some kinetic parameters as possible changes of the adsorption rates in function of the initial concentration and the adsorption time, as well as the determination of fractionary kinetic orders (Lopes et al. 2003).

Three mechanistic models have been used in order to evaluate the S-IV kinetic adsorption: the Dünwald-Wagner intraparticle diffusion model; the film-diffusion model of Boyd, which assumes that the main resistance to diffusion is in the boundary layer surrounding the adsorbent particle, and the model of Weber-Morris. The models of Dünwald-Wagner and Boyd are typically expressed as shown in Eq. 10 (Malash and El-Khaiary 2010b; Rincón-Silva et al. 2015):

$$F = 1 - \left(\frac{6}{\pi^2}\right) \cdot \sum_{n=1}^{\infty} \left(\frac{1}{n^2}\right) \cdot \exp\left(-n^2 \cdot B \cdot t\right) \tag{10}$$

where B is a constant and F represents the fractional attainment of equilibrium (q_t/q_e) at different times of contact, t. The equation is simplified leading to the Dünwald model, which is expressed (Podder and Majumder 2016) in Eq. 11:

$$ln\left(1 - F^2\right) = -k_{DW} \cdot t \tag{11}$$

where k_{DW} represents the adsorption rate constant in the model.

Reichenberg (Malash and El-Khaiary 2010b; Podder and Majumder 2016; Reichenberg 1953; Teixeira et al. 2013) managed Eq. 10 to obtain the approximations given in Eqs. 12 and 13:

$$\text{for F} < 0.85;\quad B \cdot t = \left(\sqrt{\pi} \cdot \left(1 - \sqrt{1 - \frac{\pi \cdot F}{3}}\right)\right)^2 \tag{12}$$

$$\text{for F} > 0.85;\quad B \cdot t = -ln\left(\frac{6}{\pi^2}\right) - ln(1 - F) \tag{13}$$

Additionally, the constant B may be used to calculate the effective diffusion coefficient, Di ($cm^2\ s^{-1}$) from Eq. 14:

$$D_i = B \cdot \left(\frac{r}{\pi}\right)^2 \tag{14}$$

DEM, also used in wastewater treatment processes, is implemented in order to evaluate a two-step adsorption mechanism: (1) the rapid adsorption that takes place on available inner surfaces that are easily accessible at the initial stages of the adsorption process and (2) the slow adsorption process that occurs after, due to limitation in available surface sizes (Tosun 2012).

Most of the kinetic adsorption models have been suitably used in the prediction and modelling of other adsorption systems in the presence of activated carbon adsorbents used in wastewater treatment (Figaro et al. 2009; Mezenner and Bensmaili 2009; Rincón-Silva et al. 2015; Rodriguez et al. 2009). Kinetic and statistical parameter values of the fitted kinetic models are summarized in Table 3. According to $r^2{}_{adj}$ values, the mechanistic models Boyd-Reichenberg,

Table 3 Parameter values and statistical data obtained from the fitting of the kinetic adsorption models

Kinetic model	Parameters	PAC	PACNA	PACNAU	PACNAUT	PACHP	PACSA
Pseudo-first-order (Lagergren)	k_f (min^{-1})	0.047	0.030	0.035	0.054	0.038	0.037
	$q_{e,f}$ (mg g^{-1})	159.9	144.7	164.8	194.5	166.9	148.1
	SSE (mg^2 g^{-2})	834.7	990.7	920.0	137.8	918.7	773.8
	r^2_{adj}	0.958	0.944	0.959	0.995	0.959	0.956
Pseudo-second-order (Ho and McKay equation)	k_s (g min^{-1} mg^{-1})	3.99×10^{-4}	2.57×10^{-4}	2.73×10^{-4}	4.32×10^{-4}	3.12×10^{-4}	3.34×10^{-4}
	$q_{e,s}$ (mg g^{-1})	172.8	159.2	179.8	206.5	181.1	161.2
	SSE (mg^2 g^{-2})	201.8	239.6	140.1	260.9	147.1	129.4
	r^2_{adj}	0.957	0.962	0.980	0.954	0.976	0.975
Bangham	m	6.22	4.54	5.09	8.04	5.56	5.36
	k_r (mg g^{-1} min$^{-1/m}$)	66.15	41.77	54.80	97.56	61.28	52.33
	SSE (mg^2 g^{-2})	328.1	116.7	275.3	1568.2	333.1	211.6
	r^2_{adj}	0.983	0.993	0.987	0.945	0.985	0.988
Elovich	α (mg g^{-1} min^{-1})	111.48	22.60	48.67	273.84	82.05	57.98
	β (g mg^{-1})	0.0439	0.0375	0.0374	0.0402	0.0404	0.0436
	SSE (mg^2 g^{-2})	201.2	15.7	89.5	1334.1	163.0	81.7
	r^2_{adj}	0.957	0.998	0.988	0.770	0.976	0.985
Avrami	n_{AV}	0.424	0.431	0.479	0.901	0.477	0.455
	k_{AV} (min^{-1})	0.034	0.014	0.024	0.055	0.029	0.025
	$q_{e,AV}$ (mg g^{-1})	178.7	176.3	184.1	195.3	183.7	166.9
	SSE (mg^2 g^{-2})	147.1	5.4	7.1	137.8	41.2	27.6
	r^2_{adj}	*0.991*	*0.999*	*0.999*	*0.995*	*0.998*	*0.998*
Dünwald-Wagner intraparticle diffusion	k_{DW} (min^{-1})	0.0213	0.0120	0.0149	0.0291	0.0172	0.0163
	$q_{e,DW}$ (mg g^{-1})	164.9	151.9	171.2	197.0	172.8	153.7
	SSE (mg^2 g^{-2})	417.2	210.1	187.7	226.3	229.8	218.6
	r^2_{adj}	0.979	0.988	0.992	0.992	0.990	0.988
Boyd-Reichenberg model	B (min^{-1})	0.0136	0.0068	0.0136	0.0524	0.0136	0.0136
	$q_{e,BR}$ (mg g^{-1})	172.3	173.1	181.9	200.7	190.1	168.9
	$D_{i,r=53\ \mu m}$ (cm^2 s^{-1})	6.45×10^{-10}	3.22×10^{-10}	6.43×10^{-10}	2.48×10^{-9}	6.43×10^{-10}	6.47×10^{-10}
	$D_{i,r=125\ \mu m}$ (cm^2 s^{-1})	3.59×10^{-9}	1.79×10^{-9}	3.58×10^{-9}	1.38×10^{-8}	3.58×10^{-9}	3.60×10^{-9}
	SSE (mg^2 g^{-2})	16,889	17,979	12,420	423	14,734	11,056
	r^2_{adj}	0.688	0.694	0.783	0.994	0.743	0.757
Weber-Morris intraparticle diffusion	k_{id} (mg g^{-1} min$^{-1/2}$)	4.08	4.73	4.91	3.77	4.63	4.26
	C (mg g^{-1})	92.96	63.20	80.93	130.26	88.67	76.35
	SSE (mg^2 g^{-2})	710.8	413.2	756.7	2431.9	830.1	577.9
	r^2_{adj}	0.700	0.830	0.778	0.557	0.742	0.761
Double-exponential model (DEM)	k_2 (min^{-1})	0.014	0.010	0.013	0.053	0.014	0.013
	D_2/m_a (mg g^{-1})	4.5	4.6	4.7	5.2	4.6	4.5
	$q_{e,DEM}$ (mg g^{-1})	169.0	155.4	173.6	194.7	175.3	156.6
	SSE (mg^2 g^{-2})	321.3	66.4	92.7	137.0	114.6	125.9
	r^2_{adj}	0.768	0.842	0.851	0.994	0.835	0.824

Weber-Morris and DEM are the less appropriate kinetic models to predict the adsorption of S-IV onto the modified activated carbons used. The only mechanistic kinetic model capable of predicting reasonably well the experimental data with all materials is the Dünwald-Wagner model (r^2_{adj} higher than 0.979). Exceptionally, the models of Boyd-Reichenberg and DEM are capable of predicting suitably the experimental data obtained with the highlighted adsorbent (PACNAUT), evidencing that the adsorption of S-IV onto this material takes place in a different way when compared to the other adsorbents. In fact, as can be observed in Fig. 1, the removal of S-IV with PACNAUT happens rapidly at a first stage in the adsorption run, describing a pronounced knee when the asymptotic limit is reached, whereas the knee of the adsorption curve obtained with the other materials is not so pronounced. The most significant difference between PACNAUT and the other adsorbents tested is the thermal treatment up to 800 °C performed after the chemical treatments. This leads to a significant decrease of the superficial oxygen groups on the surface of the material (Gomes et al. 2010; Ribeiro et al. 2013), which may be found to affect strongly the adsorption process in the liquid phase (Álvarez et al. 2015). In fact, the effective diffusion coefficient (D_i) obtained from the Boyd-Reichenberg model for the adsorption run carried out with the PACNAUT adsorbent was remarkably higher (0.248–1.38 × 10^{-8} cm^2 s^{-1}) than the value obtained with the other adsorbents (0.322–3.60 × 10^{-9} cm^2 s^{-1}), evidencing a more effective diffusion when PACNAUT is used (a D_i value range was obtained taking into consideration the two available particle radius of the sieving performed).

The remaining fitted kinetic models (pseudo-first-order, pseudo-second-order, Bangham, Elovich, and Avrami) allow a suitable simulation of the adsorption process, since r^2_{adj} takes values higher than 0.9441–0.9995, with the only exception being found for the Elovich model applied to the experimental data obtained with PACNAUT adsorbent (r^2_{adj} was found to be 0.770, respectively). This also evidences a completely different behaviour in the adsorption of S-IV with the other adsorbents. All kinetic constants (k_f, k_s, k_r, α, k_{AV}, k_{DW}, B and k_2) and equilibrium capacity (q_e) from these models are considerably higher when S-IV is taken up onto the thermally treated activated carbon (PACNAUT).

To the best of our knowledge, there is only one work dealing with the adsorption of S-IV for treatment of wastewater (Sun et al. 2015). In that report, the kinetic adsorption on magnetic carbon nanotubes was assessed by applying the pseudo-first- and pseudo-second-order model and the kinetic coefficients were slightly higher than the values obtained here ($k_f = 0.063$ min^{-1} and $k_s = 1.022$ g mg^{-1} min^{-1}). However, the adsorption capacity was considerably lower when compared to the PACNAUT adsorbent ($q_{e,experimental} = 0.921$ mg g^{-1}, $q_{e,f} = 0.412$ mg g^{-1} and $q_{e,s} = 0.908$ mg g^{-1}). The kinetic constant values are higher when compared to the results obtained in the dye adsorption onto other activated carbon adsorbents. For instance, in the adsorption of methylene blue and Orange II from aqueous solutions, the following values were obtained: $k_r = 35.33$ mg g^{-1} $min^{-1/(m = 0.124)}$ and 0.221 mg g^{-1} $min^{-1/(m = 1.83)}$, $\alpha = 52.36$ mg g^{-1} min^{-1} and 57.09 (applying the assumption of Chien and Clayton) and $k_{id} = 8.08$ and 1.00 mg g^{-1} $min^{-0.5}$ ($r^2 > 0.906$ for both pollutants and all models) at 40 °C, respectively (Rodriguez et al. 2009). In the adsorption of Indigo Carmine from aqueous solution onto granular activated carbon, the following kinetic constant values were obtained: $k_f = 0.000148$ min^{-1}, $k_s =$ 0.0000651 g min^{-1} mg^{-1}, $\alpha = 0.06$ mg g^{-1} min^{-1} (applying the assumption of Chien and Clayton) and $k_{id} =$ 0.387 mg g^{-1} $min^{-0.5}$ (Secula et al. 2011) (considering the highest values obtained in the operating conditions explored). In addition to the kinetic and equilibrium adsorption, other parameters show also remarkable values for the PACNAUT adsorbent when compared to the other tested adsorbents in this work. The parameter m of the Bangham equation, which may be used as indicator of the adsorption intensity (Rodriguez et al. 2009), takes the value of 8.04 for the adsorption performed on the PACNAUT adsorbent, whereas m reaches values from 4.54 to 6.22 for the other adsorbents. In any case, the value of m was higher than the previous study regarding the adsorption of methylene blue and Orange II.

The equation from Avrami model shows the best statistical parameter ($r^2_{adj} \geq 0.991$ and $SSE \geq 0.279$) to represent the adsorption of S-IV onto all activated carbons tested; hence, the Avrami model was the most suitable equation to describe the adsorption kinetics. Figure 2 shows the parity plot of q_t values predicted with the Avrami model compared to the experimental q_t values (inlet showing as normalized concentrations of S-IV, $C_{S\text{-}IV}/C_{S\text{-}IV,0}$). As can be observed, the experimental q_t values agreed very well with the calculated values (Figs. 1 and 2). The equation of the Avrami kinetic model presents the Avrami exponential (n_{AV}) that is a fractionary number related with the possible changes of the adsorption mechanism that takes place during the adsorption process (Lopes et al. 2003). The factor order obtained in the fitting of the Avrami equation to the data obtained from adsorption onto PACNAUT is found to be near to 1, in opposition to that obtained with all other adsorbents (n_{AV} is ca. 0.5). The equilibrium adsorption capacity values determined from the Avrami model ($q_{e,AV}$) are nearest to the experimental values of q_{24h} for all runs regardless of the modified or unmodified activated carbons. According to the rate constant (k_{AV}) from

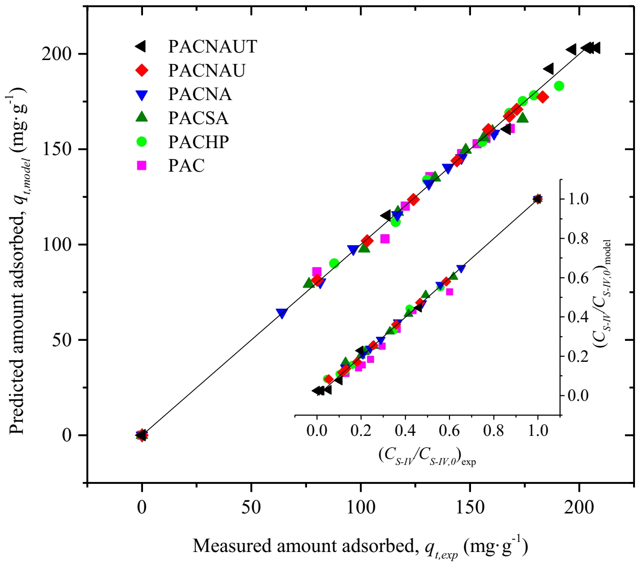

Fig. 2 Parity plots of amount adsorbed of S-IV measured for each material and predicted from the Avrami model (Inlet: representation of the normalized concentration)

the Avrami model, the adsorbents can be screened (in the order of descending adsorption rate value) as follows: PACNAUT > PAC > PACHP > PACSA > PACNAU > PACNA. In this sense, the thermal and chemical modified carbon (PACNAUT) is the most effective adsorbent regarding fast adsorption in lipophilic pollutant-biphasic mixture systems.

Other works related to the adsorption of organic pollutants from aqueous solutions onto activated carbon adsorbents also conclude that the Avrami model is the most appropriate model to represent the experimental data (Oladoja 2015; Wang 2012).

Adsorption isotherms

Figure 3 shows the adsorption isotherm curves of S-IV in the presence of all modified and unmodified powdered activated carbon adsorbents. The results show a similar shape curve with all the activated carbons, the q_e values not describing an asymptotic curve. Instead, a progressive increment of the q_e values is observed with the increase of the equilibrium pollutant concentration (C_e) in the organic phase, revealing likely the formation of successive layers of adsorbate onto the activated carbons at higher pollutant concentrations.

Interestingly, the observed increasing slope of the curve upon the increase of pollutant concentration in the equilibrium is similar for all adsorbents tested. However, a significant difference can be observed for the lowest C_e values, for which the q_e takes values completely different for each adsorbent. Based on this, the adsorption isotherm can be classified as L1 or H1, according to the Giles classification (Giles et al. 1960; Giles et al. 1974). The L shape means that there is no strong competition between solvent and the adsorbate to occupy the adsorbent surface sites (Hamdaoui and Naffrechoux 2007a). In this case, the L1 may be associated to activated carbons with less affinity for S-IV (PACNA-PACNAU). That affinity was changed with the different treatments used to modify the PAC material, to achieve a significant increment with the PACNAUT that describes an H1 isothermal adsorption type and shows the highest amount of S-IV adsorbed in the equilibrium stage. The H1 isothermal adsorption is typically found when the adsorbate and adsorbent show a strong affinity with each other. L shape curve is more reported in other works regarding dye adsorption on activated carbon (Ai et al. 2010; Malik 2003) (there are no reported works about this classification or isothermal adsorption studies of S-IV).

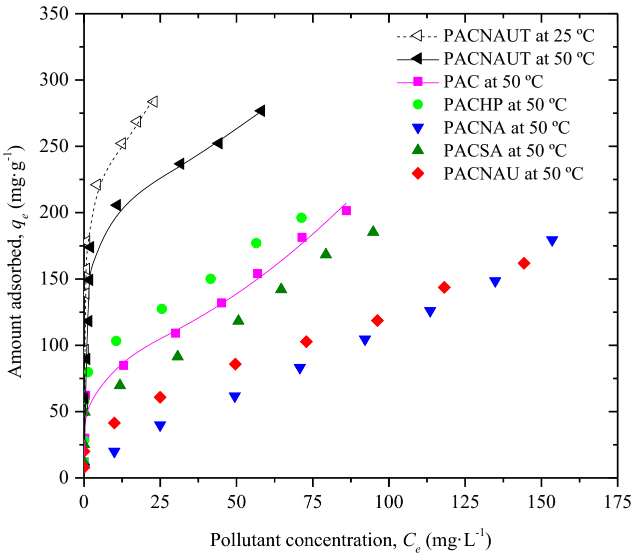

Fig. 3 Adsorption isotherm curves of Sudan-IV (experimental values as symbols and as curves values predicted by multilayer Jovanović model) with the different activated carbons. Operating conditions: biphasic mixture W/O = 1:10 of water/cyclohexane, natural pH, 50 °C, $C_{S\text{-}IV,0}$ = 500 mg L^{-1}, $C_{adsorbent}$ = 2.5 g L^{-1} of organic phase and a contact time of 48 h

There are several equations to analyse and model experimental adsorption equilibrium results. The most accepted surface adsorption models for single-solute systems are the Langmuir (Langmuir 1918) and Freundlich (Freundlich 1907) models. However, other isotherm models allow improving the simulation of experimental adsorption equilibrium data and the physical interpretation of the model parameters. Here, an extensive number (14) of adsorption isotherm models (Table 4) is evaluated in order to predict suitably the adsorption of S-IV on the PACNAUT adsorbent and on the parent commercial powdered activated carbon (PAC), used as references. The selected adsorption isotherm models are commonly used to predict the removal of a single pollutant from one-phase wastewater on activated carbons (Mezenner and Bensmaili 2009; Rodriguez et al. 2009). The model and statistical parameter values obtained from the application of the adsorption isotherm model equations are collected in Table 5. The majority of the adsorption isotherm models, especially the empirical models, are based on the division of polynomial equations, being thus possible to describe a mathematical relationship between them (Fig. 4). In this work, all adsorption isotherm models were explored to study the consideration of more coefficient parameters (discussed based on the adjusted r^2).

The q_m values of 183.0 and 258.2 mg g^{-1} obtained in the Langmuir model with PAC and PACNAUT, respectively, are close to the experimental values of q_m (201 and 276 mg g^{-1}). The separation factor (R_L), calculated according to Eq. 15, is typically used to verify if the adsorption in the studied system is unfavourable ($R_L > 1$), linear ($R_L = 1$), favourable ($0 < R_L < 1$) or irreversible ($R_L = 0$).

$$R_L = \frac{1}{1 + K_L \cdot C_0} \tag{15}$$

In the initial S-IV concentration range studied (30–600 and 150–750 mg L^{-1} with PAC and PACNAUT, respectively), the

Table 4 Adsorption isotherm models

Isotherm models	Non-linear form	Parameters
Langmuir	$q_e = \frac{q_{m,L} \cdot K_L \cdot C_e}{1+K_L \cdot C_e}$	$q_{m,\ L}$, K_L
Freundlich	$q_e = K_F \cdot C_e^{1/n_F}$	K_F, n_F
Redlich-Peterson or Radke-Prausnitz (RP models)	$q_e = \frac{A_{RP} \cdot C_e}{1+B_{RP} \cdot C_e^g}$	A_{RP}, B_{RP}, g
Khan	$q_e = \frac{q_{m,K} \cdot a \cdot C_e}{(1+a \cdot C_e)^b}$	$q_{m,\ K}$, a, b
Sips	$q_e = \frac{q_{m,S} \cdot K_S \cdot {C_e}^n}{1+K_S \cdot {C_e}^n}$	$q_{m,\ S}$, K_S, n
Tóth	GIE for $K_1 > K$: $q_e = \frac{q_{m,To} \cdot C_e}{\left(1/K_{To}+C_e^{n_{To}}\right)^{1/n_{To}}}$	$q_{m,\ To}$, K_{To}, n_{To}
	GIE: $q_e = \frac{q_{m,To} \cdot a \cdot C_e^{ma}}{1+a \cdot C_e^{ma}-k \cdot C_e^{m_k}}$	$q_{m,\ To}$, a, k, m_a, m_k
Fritz-Schlunder (single solute)	$q_e = \frac{\left(\frac{a_{10}}{c_1}\right) \cdot C_e^{b_{10}}}{1+\left(\frac{a_{11}}{c_1}\right) \cdot C_e^{b_{11}}}$	$\left(\frac{a_{10}}{c_1}\right)$, $\left(\frac{a_{11}}{c_1}\right)$, b_{10}, b_{11}
Vieth-Sladek	$q_e = K_{VS} \cdot C_e + \frac{q_{m,VS} \cdot \beta_{VS} \cdot C_e}{1+\beta_{VS} \cdot C_e}$	K_{VS}, $q_{m,\ VS}$, β_{VS}
Guggenheim-Anderson-de Boer (GAB)	$q_e = \frac{q_{m,GAB} \cdot c \cdot K \cdot C_e}{(1-K \cdot C_e) \cdot [1+(c-1) \cdot K \cdot C_e]}$	$q_{m,\ GAB}$, K, c
Harkins-Jura	$q_e = \left(\frac{A_{HJ}}{B_{HJ}-\log(C_e)}\right)^{1/2}$	A_{HJ}, B_{HJ}
Tempkin	$q_e = \frac{R \cdot T}{b_T} \cdot \ln(K_T \cdot C_e)$	b_T, K_T
Dubinin–Radushkevich	$q_e = q_{m,\ DR} \cdot (\exp(-K_{DR} \cdot (\varepsilon)^2))$ $\varepsilon = R \cdot T \cdot \ln\left(1 + \frac{1}{C_e}\right)$	$q_{m,\ DR}$, K_{DR}
Brouers-Sotolongo	$q_e = q_{m,BS} \cdot \left(1-\exp\left(-K_{BS} \cdot C_e^{\alpha}\right)\right)$	q_m, K_{BS}, α
Jovanović	For monolayer: $q_e = q_{m,\ J} \cdot (1 - \exp(-K_J \cdot C_e))$ For multilayer: $q_e = q_{m,\ J} \cdot (1 - \exp(-K_J \cdot C_e)) \cdot \exp(K'_J \cdot C_e)$	$q_{m,\ J}$, K_J, K'_J

values obtained (Fig. 5) show a favourable adsorption of S-IV from the organic phase on PAC and PACNAUT. The decrease in R_L with the increase of the initial concentration indicates that the adsorption is more favourable at high concentrations of S-IV.

The values obtained of the heterogeneity factor for the Freundlich isotherm model with PAC ($n_F = 2.83$) and PACNAUT ($n_F = 4.73$) indicate that adsorption is physical, since n_F values obtained were more than 1 (Rincón-Silva et al. 2015).

The Redlich–Peterson isotherm was developed to improve the fitting between the Langmuir and the Freundlich equations (Redlich and Peterson 1959) and, few years later, Radke and Prausnitz developed an identical mathematical model studying the adsorption of organic solutes from dilute aqueous solutions on activated carbon (Radke and Prausnitz 1972). The Radke-Prausnitz isotherm model can be found expressed in different forms, which were summarized in three different isotherms by some authors (Hamdaoui and Naffrechoux 2007b; Saadi et al. 2015). However, the function reported by Radke and Prausnitz was expressed as shown in Eq. 16:

$$\frac{1}{n_i^c} = \frac{1}{a \cdot c_i} + \frac{1}{b \cdot c_i^{\beta}} \qquad (16)$$

where n_i^c refer the moles of adsorbed solute on the adsorbent per gram (q_e), c_i the concentration of the adsorbate in the liquid solution (mol/L) and a, b and β are constant parameters of the model. The expression can be transformed as given in Eq. 17.

$$q_e = \frac{a \cdot c_i}{1 + \left(\frac{a}{b}\right) \cdot c_i^{1-\beta}} \qquad (17)$$

Thus, the expression can be considered mathematically identical to the Redlich–Peterson isotherm ($a \approx A_{RP}$, $a/b \approx B_{RP}$ and $1\text{-}\beta \approx g$, as presented in Table 4). Here, both isotherm models were named RP model. Detailed discussion about the results obtained with the RP, Khan, Sips, Fritz and Schluender, Guggenheim, Anderson and de Boer (GAB), Harkins–Jura

Table 5 Parameter values and statistical data obtained from the fitting of the adsorption isotherm models

Isotherm models	Parameter model	PAC	PACNAUT	Statistical parameter	PAC	PACNAUT
Langmuir	$q_{m,L}$ (mg g^{-1})	183.0	258.2	SSE (mg^2 g^{-2})	6828	2726
	K_L (L mg^{-1})	0.024	0.720	r^2	0.864	0.944
				r^2_{adj}	0.842	0.937
Freundlich	K_F (mg^{n+1} g^{-1} L^{-n})	38.0	117.1	SSE (mg^2 g^{-2})	2145	3134
	n_F	2.83	4.73	r^2	0.941	0.932
	$(1/n_F)$	0.354	0.212	r^2_{adj}	0.933	0.922
RP models	A_{RP} (L g^{-1})	6.69	395.3	SSE (mg^2 g^{-2})	5297	1715
	B_{RP} (L^g mg^{-g})	0.101	2.409	r^2	0.958	0.962
	g	0.649	0.878	r^2_{adj}	0.944	0.950
Khan	$q_{m,K}$ (mg g^{-1})	101.6	139.5	SSE (mg^2 g^{-2})	4725	1727
	a (L mg^{-1})	0.101	2.427	r^2	0.938	0.962
	b	0.675	0.868	r^2_{adj}	0.917	0.950
Sips	$q_{m,S}$ (mg g^{-1})	205.7	277.8	SSE (mg^2 g^{-2})	4909	4432
	K_S (L^n mg^{-n})	0.301	0.534	r^2	0.861	0.958
	n	0.552	0.645	r^2_{adj}	0.815	0.945
Tóth-$K_1 > K$	$q_{m,To}$ (mg g^{-1})	238.6	327.7	SSE (mg^2 g^{-2})	4823	1807
	K_{To} (L^{nTo} mg^{-nTo})	4.191	3.052	r^2	0.863	0.960
	n_{To}	0.364	0.433	r^2_{adj}	0.817	0.947
Tóth-GIE	$q_{m,To}$ (mg g^{-1})	66.9	245.7	SSE (mg^2 g^{-2})	195	1358
	a (L^{ma} mg^{-ma})	15.80	0.876	r^2	0.994	0.970
	k (L^{mk} mg^{-mk})	1.211	$1.0 \cdot 10^{-5}$	r^2_{adj}	0.989	0.941
	m_a	1.949	0.788			
	m_k	2.438	3.127			
Fritz-Schlunder (single solute)	(a_{10}/c_1) (mg g^{-1}·L^{b10}/mg^{b10})	40.4	339.0	SSE (mg^2 g^{-2})	2144	1705
	(a_{11}/c_1) (L^{b11}/mg^{b11})	0.064	1.934	r^2	0.941	0.963
	b_{10}	0.354	0.901	r^2_{adj}	0.906	0.940
	b_{11}	0.000	0.793			
GAB	$q_{m,GAB}$ (mg g^{-1})	92.2	212.3	SSE (mg^2 g^{-2})	589.2	1564
	c	384.6	282.9	r^2	0.984	0.967
	K (L mg^{-1})	$6.5 \cdot 10^{-3}$	$4.1 \cdot 10^{-3}$	r^2_{adj}	0.978	0.956
Vieth-Sladek	$q_{m,VS}$ (mg g^{-1})	66.7	208.0	SSE (mg^2 g^{-2})	388.9	1557
	K_{VS} (L g^{-1})	$1.5 \cdot 10^{-3}$	$1.2 \cdot 10^{-3}$	r^2	0.989	0.967
	β_{VS} (L mg^{-1})	4.475	1.209	r^2_{adj}	0.985	0.956
Harkins-Jura	A_{HJ} (mg^2 g^{-2})	$6.9 \cdot 10^3$	$3.5 \cdot 10^4$	SSE (mg^2 g^{-2})	2089	6766
	B_{HJ}	2.09	2.19	r^2	0.952	0.858
				r^2_{adj}	0.945	0.838
Tempkin	$R \cdot T \cdot (b_T)^{-1}$ (mg g^{-1})	22.7	37.3	SSE (mg^2 g^{-2})	4669	1854
	b_T (g·J·mg^{-1} mol^{-1})	61.7	99.3	r^2	0.866	0.959
	K_T (L mg^{-1})	15.03	22.91	r^2_{adj}	0.847	0.953
Dubinin–Radushkevich	$q_{m,DR}$ (mg g^{-1})	169.7	241.9	SSE (mg^2 g^{-2})	8489	6995
	$K_{DR} \cdot R^2 \cdot T^2$	164.0	2.19	r^2	0.855	0.900
				r^2_{adj}	0.835	0.885
Brouers-Sotolongo	$q_{m,BS}$ (mg g^{-1})	201.0	271.3	SSE (mg^2 g^{-2})	3902	2070
	K_{BS} (L$^{\alpha}$ mg$^{-\alpha}$)	0.228	0.544	r^2	0.891	0.955
	α	0.354	0.443	r^2_{adj}	0.855	0.940
Jovanović-monolayer	$q_{m,J}$ (mg g^{-1})	214.7	243.2	SSE (mg^2 g^{-2})	5549	4229
	K_J (L mg^{-1})	0.025	0.535	r^2	0.939	0.918
				r^2_{adj}	0.930	0.906

Table 5 (continued)

Isotherm models	Parameter model	PAC	PACNAUT	Statistical parameter	PAC	PACNAUT
Jovanović-multilayer	$q_{m,J}$ (mg g^{-1})	78.8	193.6	*SSE* (mg^2 g^{-2})	218	1607
	K_J (L mg^{-1})	2.371	0.796	r^2	*0.994*	*0.971*
	K'_J (L mg^{-1})	0.011	$6.1\cdot10^{-3}$	r^2_{adj}	*0.992*	*0.961*

and Tempkin models can be found in the Supplementary Material.

The Tóth isotherm model comes from the development of Tóth in a general isotherm equation (GIE) to model all types of isotherms taking into account the heterogeneity and the lateral and vertical interaction energies of the adsorbed molecules. The Tóth isotherm model normally used in the modelling of one-phase wastewater treatment by adsorption is the solution of the GIE when the dynamic equilibrium adsorption is higher for the monolayer than the subsequent formed layers ($K_1 > K$ as Tóth notation), which was successfully found to describe type I gas isotherms, as Tóth explained (Tóth 1981). The values of q_m found in the fit of the simplified Tóth isotherm—$K_1 > K$ (238.6 and 327.7 mg g^{-1} with PAC and PACNAUT adsorbents, respectively) were those more distant to the experimental data amongst all the isotherm models studied. The solution of the Tóth isotherm for $K_1 > K$ is not appropriate for the adsorption isotherms of S-IV, because the solution of the GIE with $K_1 > K$ describes a horizontal asymptote. For this reason, the explicit GIE proposed by Tóth was adapted in this work to be used in the adsorption of the S-IV from the biphasic liquid system, as given in Eq. 18.

$$q_e = \frac{q_{To}\cdot a\cdot C_e^{m_a}}{1+a\cdot C_e^{m_a}-k\cdot C_e^{m_k}} \tag{18}$$

where q_{To} is a constant measured in mg g^{-1}, A and K are constants (L$^{\text{ma}}$·mg$^{-\text{ma}}$ and L$^{\text{mk}}$·mg$^{-\text{mk}}$, respectively), and m_a and m_k are exponents, which can take values in a wide range (> 0), allowing to predict suitably different shapes of adsorption isotherms. S1, S2, L1 and L2 types according to the Giles classification may be modelled appropriately for $m_a, m_k \geq 1$, $m_a > 1$ and $0 \leq m_k \leq 1$, $0 \leq m_a \leq 1$ and $m_k \geq 1$, and $m_a, m_k \leq 1$, respectively. As consequence of the versatility of this model (Fig. 4), it is used as one of the check models that are able to predict highly suitable the experimental data.

The Jovanović model describes an isotherm adsorption for monolayer and multilayer physical adsorption. It was developed initially for gas adsorption (Jovanović 1969), but it is largely used in the adsorption of adsorbates from one-phase aqueous solutions (Hadi et al. 2010; Vargas et al. 2011; Wang

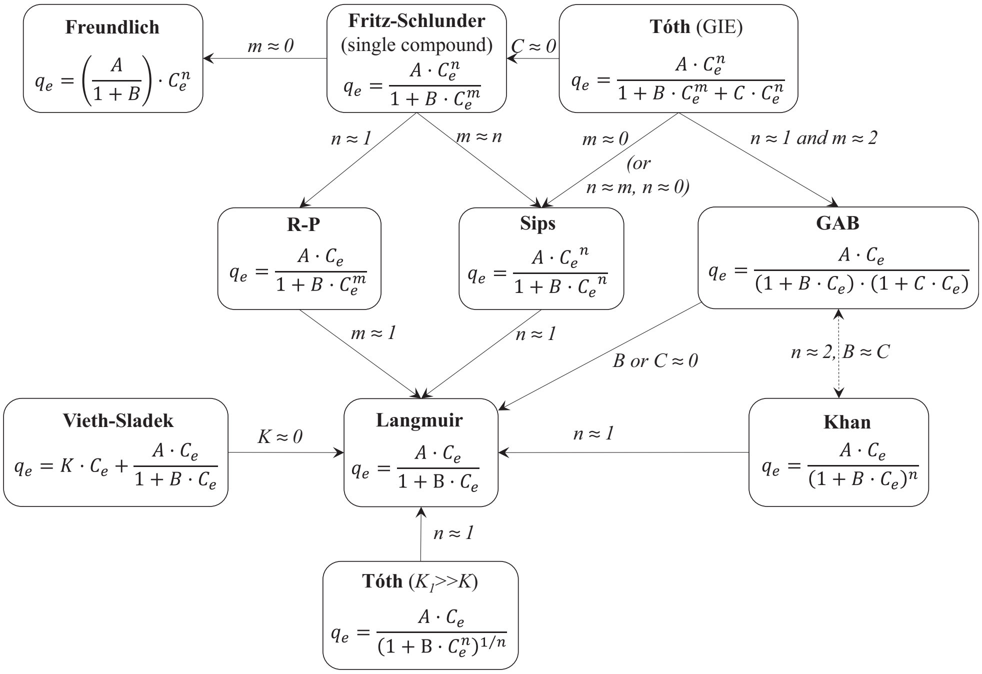

Fig. 4 Generic expressions of the adsorption isotherm models and relationships between them

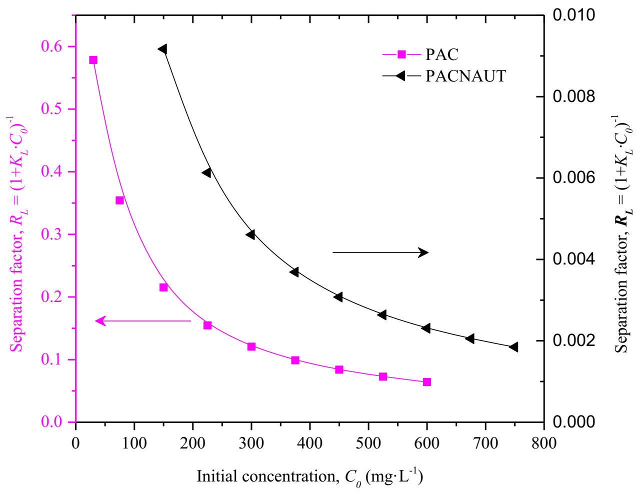

Fig. 5 Langmuir separation factor obtained in the adsorption experiments S-IV onto PAC and PACNAUT samples

2012). This isotherm adsorption model was found to present the best statistical parameters in terms of *SSE*, r^2 and r^2_{adj} when multilayer adsorption is considered. In fact, the Jovanović model is able to predict most suitably the experimental data when compared with other isotherm models based on multilayer form (e.g. the Harkins Jura or GAB models). This shows that the Jovanović multilayer isotherm can be satisfactorily used in the adsorption of S-IV onto activated carbonaceous materials. Data predicted with the model versus experimental data were represented in order to show how the model is able to adjust adequately the results (Fig. 6). Additionally, Fig. 3 shows the values of q_e predicted from application of the Jovanović isotherm with PAC and PACNAUT adsorbents. The values of q_m obtained in the fitting procedure (0.215 and 0.243 mg g^{-1} with PAC and PACNAUT, respectively) were found to be near to the experimental data. The value of q_m obtained with the unmodified activated carbon (PAC) is lower than that obtained with the modified activated carbon (PACNAUT). Similar values of the constant K_J have been obtained in other works regarding the adsorption of pollutants on activated carbon (Hadi et al. 2010; Quesada-Peñate et al. 2009). Note that the constant may take negative values in some works, as consequence of how the isotherm equations are expressed in respect to the inlet exponential content (here, it was expressed as an exponential of the constant multiplied by the equilibrium concentration, in order to obtain positive values).

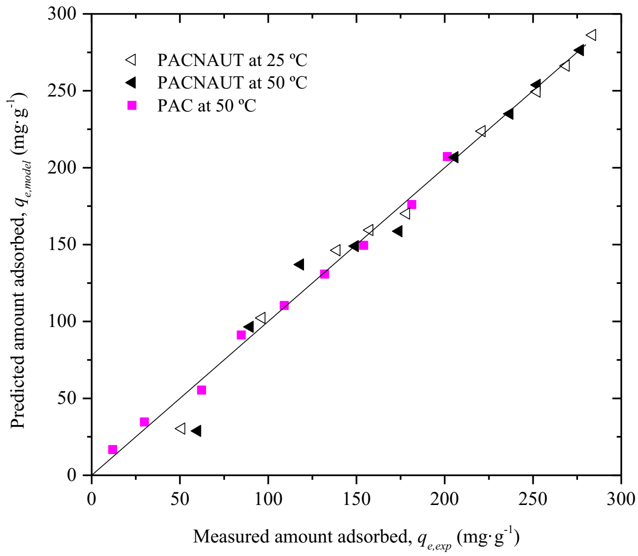

Fig. 6 Parity plot of the amount adsorbed of S-IV in equilibrium modelled by the multilayer Jovanović model

From the analysis of all the isotherms and from the knowledge of the most important parameters (q_m, *SRE* and r^2_{adj}), the isotherm models studied can be ordered according to their efficiency to predict the experimental behaviour of the S-IV adsorption onto activated carbon materials. With respect to q_m (in descending order for the modified activated carbon, PACNAUT): Tóth-K1 > K > Sips ~ Brouers-Sotolongo > Langmuir > Jovanović-monolayer ~ Dubinin–Radushkevich > Tóth-GIE > GAB ~ Vieth-Sladek > Jovanović-multilayer > Fritz Schlunder > RP > Khan. The models able to predict more suitably the experimental data ($r^2 > 0.96$), viz. Tóth-GIE ~ Jovanović-multilayer > GAB ~ Vieth-Sladek > Fritz-Schulunder > RP ~ Khan lead to q_m values between 245.7 mg g^{-1} (Tóth-GIE) and 164 mg g^{-1} (RP). Thus, the adsorption capacity of the monolayer for the PACNAUT material is expected to be found in this range of values, being 193.6 mg g^{-1} for the isotherm model that better fits the experimental data (Jovanović-multilayer). As can be appreciated in Table 5, and as expected, the q_m values obtained through the fitting of the experimental data with PACNAUT are higher than the values obtained with PAC for all the fitted equations from adsorption isotherm models.

To the best of our knowledge, there are no studies regarding the modelling of the adsorption of S-IV on lipophilic activated carbons from biphasic liquid systems simulating oily wastewater effluents. The saturated adsorption capacity (q_m) of S-IV achieved with multi-walled carbon nanotubes with S-IV molecularly imprinted polymers (MWNTs-MIPs), used as adsorbents to detect the pollutant by analysis techniques, was found to be 24.4 mg g^{-1} (Zhang et al. 2010). In another study (Sun et al. 2015), dealing with the removal of different Sudan dyes from an aqueous solution by magnetic carbon nanotubes, a maximum adsorption of 18.8679 mg g^{-1} was achieved with S-IV at 45 °C (determined from the Langmuir isotherm model). A part of other study (Li et al. 2014) reveals that it is possible to achieve an adsorption equilibrium of S-IV (970.87 μg g^{-1}) onto ferromagnetic titanium dioxide nanoparticles (determined by the pseudo-second-order kinetic adsorption). However, the aim of those works was not the treatment of wastewater or polluted organic solvents. Chang et al. studied the adsorption and photocatalytic degradation of different Sudan dyes reaching a maximum adsorption of 20 mg g^{-1}

onto TiO_2@MIL-53 core-shell composites (Chang et al. 2016). The adsorption of Sudan dyes was not modelled in that work.

Effect of temperature and thermodynamic study

The adsorption of S-IV with the best material (PACNAUT) was also explored at low temperature (25 °C) in order to investigate the effect of this parameter and to study briefly the thermodynamics of this process. The adsorption isotherm at 25 °C is depicted in Fig. 3. As can be observed, the amount of S-IV adsorbed on the PACNAUT material is higher at 25 °C when compared to 50 °C. The curve obtained at 25 °C was also modelled with the Jovanović equation, resulting in a good accuracy of the predicted values, $r^2 = 0.987$ (Fig. 6). At that temperature, model took higher values for the equilibrium constants ($K_J = 1.916$ L mg^{-1} and $K'_J = 0.0132$ L mg^{-1}), meaning that the equilibrium is more favourable to adsorb the S-IV on the PACNAUT. Thermodynamic considerations of an adsorption process are necessary to establish whether the process is spontaneous and feasible or not. Thermodynamic parameters, i.e. heat of adsorption (ΔH), free energy change (ΔG) and entropy change (ΔS), are typically calculated in adsorption studies in one-phase aqueous solutions (Maksin et al. 2012; Rodriguez et al. 2009; Wang 2012). However, it is possible to find different methodologies to estimate those parameters (Anastopoulos and Kyzas 2016). Here, the enthalpy (ΔH) was determined considering the Van't Hoff equation (Eq. 19) for the first equilibrium constant of Jovanović (K_J):

$$\frac{d\ln(K_L)}{dT}=\frac{\Delta H}{R\cdot T^2}\rightarrow\ln\left(\frac{K_{L,2}}{K_{L,1}}\right)=-\frac{\Delta H}{R}\left(\frac{1}{T_2}-\frac{1}{T_1}\right)\tag{19}$$

The free energy (ΔG) and entropy (ΔS) of adsorption were calculated according to Eqs. 20 and 21:

$$\Delta G=-R\cdot T\cdot\ln(K)\tag{20}$$

$$\Delta S=\frac{\Delta H-\Delta G}{T}\tag{21}$$

Most studies show the use of the Langmuir constant ($K = K_L$) to calculate the Gibbs free energy, but it is also possible to find K as q_e/C_e and C_{Ae}/C_e, where C_{Ae} would be the equilibrium concentration adsorbed on adsorbent per litter of the bulk solution. Additionally, there is some controversy about the use of units for K (L mol^{-1}, L mg^{-1}, L g^{-1} or dimensionless). Obviously, the units affect the value of K, altering significantly the interpretation of the results (e.g., for unfavourable equilibrium $K < 1 \rightarrow \ln(K) < 0 \rightarrow \Delta G > 0$). The use of q_e/C_e or C_{Ae}/C_e is subjected to the operational conditions, since the q_e/C_e ratio can take different values (Fig. 3). Here, the dimensionless (fitting with C_e as mg of pollutant per mg of solution) Jovanović equilibrium constant was used for the determination of the Gibbs free energy (Table 6). However, the difference is negligible when the Langmuir constant or when L mol^{-1} were used.

The negative value of ΔH confirms the exothermic nature of the adsorption process on the material and that decreasing the temperature leads to the increase of the adsorption of S-IV on PACNAUT. Sun et al. (Sun et al. 2015) also found exothermic adsorption processes of different Sudan dyes in aqueous solution. The low value obtained for the enthalpy of adsorption indicates the physical character of the process. The negative values of the Gibbs free energy and the positive value of entropy are consistent with a spontaneous process coupled with the loss of freedom of the adsorbate molecules. However, the magnitude of the values is found inside the typical range of values reported in the literature (Anastopoulos and Kyzas 2016).

Conclusions

Successive treatments of the commercial activated carbon Norit ROX 0.8 in powder form (PAC), namely with nitric acid and urea, followed by a thermal treatment at 800 °C under inert atmosphere, resulted in the sample PACNAUT, which revealed the highest adsorption performance amongst all materials tested ($q_e = 200$ mg g^{-1} with 2.5 g L^{-1} of PACNAUT and 500 mg of S-IV per litter of organic phase). Due to the lipophilic character of both adsorbent and adsorbate, the effect of water is negligible in the adsorption of S-IV contained in a mixture of oil-water. Then, it is possible for the use of one-liquid-phase kinetic and adsorption isotherm models to predict their behaviour in the static adsorption of pollutants present in wastewater effluents with no more considerations. Rectifications of some models gathered from literature have been done to employ them correctly in the modelling of the adsorption of S-IV on the developed materials. Kinetic ad equilibrium constants take higher values for PACNAUT when compared with the other materials tested, revealing that hydrothermal modifications allow increasing significantly the performance of the original material. The kinetic adsorption of S-IV onto the developed materials was well-modelled by the Avrami equation (adjusted r^2 above 0.990), obtaining kinetic constants of 0.034 and 0.055 min^{-1} with PAC and PACNAUT materials, respectively, putting in evidence the

Table 6 Main parameter coefficients of the Jovanović model at 25 and 50 °C and thermodynamic constants of the adsorption of Sudan-IV on PACNAUT

Temperature (°C)	K_J (kg kg^{-1})	ΔG (kJ mol^{-1})	ΔH (kJ mol^{-1})	ΔS (kJ mol^{-1} K^{-1})
25	1.92×10^6	− 36.3	− 2.2	0.10
50	7.96×10^5	− 33.9		

more than 60% increase as consequence of the chemical and thermal treatments. On the other hand, the adsorption isotherm of S-IV on PACNAUT and PAC activated carbons is well-modelled by using the GIE of Tóth and the Jovanović expression for multilayer (r^2 above 0.97 for both models). These models are not typically used in other works reported in the literature. Generally, the Jovanović model is only employed considering the adsorption in the monolayer and the GIE Tóth expression is not used, despite its versatility to model easily isotherm curves of adsorption. In the adsorption of S-IV onto PAC and PACNAUT, the extended models allow to predict a monolayer uptake capacity greatly higher for the modified material when compared to the commercial carbon (193.6 and 78.8 mg g^{-1}, respectively, according to the Jovanović expression for multilayer adsorption). The adsorption isotherm of S-IV with PACNAUT at 25 °C confirms that the adsorption of S-IV can be increased at lower temperatures.

Funding information This work is a result of Project "AIProcMat@N2020—Advanced Industrial Processes and Materials for a Sustainable Northern Region of Portugal 2020," with the reference NORTE-01-0145-FEDER-000006, supported by Norte Portugal Regional Operational Programme (NORTE 2020), under the Portugal 2020 Partnership Agreement, through the European Regional Development Fund (ERDF); Associate Laboratory LSRE-LCM (UID/EQU/50020/2019) funded by national funds through FCT/MCTES (PIDDAC); and CIMO (UIDB/00690/2020) through FEDER under Program PT2020.

References

Abousnina RM, Nghiem LD, Bundschuh J (2014) Comparison between oily and coal seam gas produced water with respect to quantity, characteristics and treatment technologies: a review. Desalin Water Treat 54:1793–1808. https://doi.org/10.1080/19443994.2014.893541

Ai L, Huang H, Chen Z, Wei X, Jiang J (2010) Activated carbon/$CoFe_2O_4$ composites: facile synthesis, magnetic performance and their potential application for the removal of malachite green from water. Chem Eng J 156:243–249. https://doi.org/10.1016/j.cej.2009.08.028

Al-Futaisi A, Jamrah A, Yaghi B, Taha R (2007) Assessment of alternative management techniques of tank bottom petroleum sludge in Oman. J Hazard Mater 141:557–564. https://doi.org/10.1016/j.jhazmat.2006.07.023

Al-Ghouti MA, Khraisheh MA, Ahmad MN, Allen S (2009) Adsorption behaviour of methylene blue onto Jordanian diatomite: a kinetic study. J Hazard Mater 165:589–598. https://doi.org/10.1016/j.jhazmat.2008.10.018

Álvarez S, Ribeiro RS, Gomes HT, Sotelo JL, García J (2015) Synthesis of carbon xerogels and their application in adsorption studies of caffeine and diclofenac as emerging contaminants. Chem Eng Res Des 95:229–238. https://doi.org/10.1016/j.cherd.2014.11.001

Anastopoulos I, Kyzas GZ (2016) Are the thermodynamic parameters correctly estimated in liquid-phase adsorption phenomena? J Mol Liq 218:174–185. https://doi.org/10.1016/j.molliq.2016.02.059

Avrami M (1939) Kinetics of phase change. I General Theory. J Chem Phys 7:1103–1112. https://doi.org/10.1063/1.1750380

Avrami M (1940) Kinetics of phase change. II Transformation-Time Relations for Random Distribution of Nuclei. J Chem Phys 8:212–224. https://doi.org/10.1063/1.1750631

Bangham DH, Burt FP (1924) The behaviour of gases in contact with glass surfaces. Proc R Soc Lond A 105:481–488. https://doi.org/10.1098/rspa.1924.0032

Boyd GE, Adamson AW, Myers LS (1947) The exchange adsorption of ions from aqueous solutions by organic zeolites. II. Kinetics1. J Am Chem Soc 69:2836–2848. https://doi.org/10.1021/ja01203a066

Chang N, He D-Y, Li Y-X, Tang Z-W, Huang Y-F (2016) Fabrication of TiO_2@MIL-53 core–shell composite for exceptionally enhanced adsorption and degradation of nonionic organics. RSC Adv 6:71481–71484. https://doi.org/10.1039/C6RA13397E

Chen G, He G (2003) Separation of water and oil from water-in-oil emulsion by freeze/thaw method. Sep Pur Tech 31:83–89. https://doi.org/10.1016/S1383-5866(02)00156-9

Chien SH, Clayton WR (1980) Application of Elovich equation to the kinetics of phosphate release and sorption in soils. Soil Sci Soc Am J 44:265–268. https://doi.org/10.2136/sssaj1980.03615995004400020013x

Cotoruelo LM, Marqués MD, Díaz FJ, Rodríguez-Mirasol J, Rodríguez JJ, Cordero T (2009a) Equilibrium and kinetic study of Congo red adsorption onto lignin-based activated carbons. Transport Porous Med 83:573–590. https://doi.org/10.1007/s11242-009-9460-8

Cotoruelo LM, Marques MD, Rodriguez-Mirasol J, Rodriguez JJ, Cordero T (2009b) Lignin-based activated carbons for adsorption of sodium dodecylbenzene sulfonate: equilibrium and kinetic studies. J Colloid Interface Sci 332:39–45. https://doi.org/10.1016/j.jcis.2008.12.031

Diaz de Tuesta JL, Silva AMT, Faria JL, Gomes HT (2018) Removal of Sudan IV from a simulated biphasic oily wastewater by using lipophilic carbon adsorbents. Chem Eng J 347:963–971. https://doi.org/10.1016/j.cej.2018.04.105

Diaz de Tuesta JL, Machado BF, Serp P, AMT S, Faria JL, Gomes HT (2019) Janus amphiphilic carbon nanotubes as Pickering interfacial catalysts for the treatment of oily wastewater by selective oxidation with hydrogen peroxide (*in press*). Catal Today. https://doi.org/10.1016/j.cattod.2019.07.012

Diya'uddeen BH, Daud WMAW, Abdul Aziz AR (2011) Treatment technologies for petroleum refinery effluents: a review. Process Saf Environ Prot 89:95–105. https://doi.org/10.1016/j.psep.2010.11.003

Doğan M, Özdemir Y, Alkan M (2007) Adsorption kinetics and mechanism of cationic methyl violet and methylene blue dyes onto sepiolite. Dyes Pigments 75:701–713. https://doi.org/10.1016/j.dyepig.2006.07.023

Dünwald H, Wagner C (1934) Methodik der Messung von Diffusionsgeschwindigkeiten bei Lösungsvorgängen von Gasen in festen Phasen. Zeitschrift für Physikalische Chemie, Abteilung B: Chemie der Elementarprozesse B24:53–58

El-Khaiary MI, Malash GF (2011) Common data analysis errors in batch adsorption studies. Hydrometallurgy 105:314–320. https://doi.org/10.1016/j.hydromet.2010.11.005

Figaro S, Avril JP, Brouers F, Ouensanga A, Gaspard S (2009) Adsorption studies of molasse's wastewaters on activated carbon: modelling with a new fractal kinetic equation and evaluation of kinetic models. J Hazard Mater 161:649–656. https://doi.org/10.1016/j.jhazmat.2008.04.006

Foo KY, Hameed BH (2010) Insights into the modeling of adsorption isotherm systems. Chem Eng J 156:2–10. https://doi.org/10.1016/j.cej.2009.09.013

Freundlich H (1907) Über die adsorption in Lösungen (adsorption in solution) vol 57U. https://doi.org/10.1515/zpch-1907-5723

García-Mateos FJ, Ruiz-Rosas R, Marqués MD, Cotoruelo LM, Rodríguez-Mirasol J, Cordero T (2015) Removal of paracetamol on biomass-derived activated carbon: modeling the fixed bed breakthrough curves using batch adsorption experiments. Chem Eng J 279:18–30. https://doi.org/10.1016/j.cej.2015.04.144

Giles CH, MacEwan TH, Nakhwa SN, Smith D (1960) 786. Studies in adsorption. Part XI. A system of classification of solution adsorption isotherms, and its use in diagnosis of adsorption mechanisms and in measurement of specific surface areas of solids. J Chem Soc:3973–3993. https://doi.org/10.1039/JR9600003973

Giles CH, Smith D, Huitson A (1974) A general treatment and classification of the solute adsorption isotherm. I. Theoretical. J Colloid Interface Sci 47:755–765. https://doi.org/10.1016/0021-9797(74)90252-5

Gomes HT, Miranda SM, Sampaio MJ, Silva AMT, Faria JL (2010) Activated carbons treated with sulphuric acid: catalysts for catalytic wet peroxide oxidation. Catal Today 151:153–158. https://doi.org/10.1016/j.cattod.2010.01.017

Gomes HT, Miranda SM, Sampaio MJ, Figueiredo JL, Silva AMT, Faria JL (2011) The role of activated carbons functionalized with thiol and sulfonic acid groups in catalytic wet peroxide oxidation. Appl Catal B 106:390–397. https://doi.org/10.1016/j.apcatb.2011.05.044

Gurses A, Dogar C, Yalcin M, Acikyildiz M, Bayrak R, Karaca S (2006) The adsorption kinetics of the cationic dye, methylene blue, onto clay. J Hazard Mater 131:217–228. https://doi.org/10.1016/j.jhazmat.2005.09.036

Hadi M, Samarghandi MR, McKay G (2010) Equilibrium two-parameter isotherms of acid dyes sorption by activated carbons: study of residual errors. Chem Eng J 160:408–416. https://doi.org/10.1016/j.cej.2010.03.016

Hamdaoui O, Naffrechoux E (2007a) Modeling of adsorption isotherms of phenol and chlorophenols onto granular activated carbon. Part I. Two-parameter models and equations allowing determination of thermodynamic parameters. J Hazard Mater 147:381–394. https://doi.org/10.1016/j.jhazmat.2007.01.021

Hamdaoui O, Naffrechoux E (2007b) Modeling of adsorption isotherms of phenol and chlorophenols onto granular activated carbon. Part II. Models with more than two parameters. J Hazard Mater 147:401–411. https://doi.org/10.1016/j.jhazmat.2007.01.023

Ho YS (2006) Review of second-order models for adsorption systems. J Hazard Mater 136:681–689. https://doi.org/10.1016/j.jhazmat.2005.12.043

Ho YS, McKay G (1999) Pseudo-second order model for sorption processes. Process Biochem 34:451–465. https://doi.org/10.1016/S0032-9592(98)00112-5

Jovanović DS (1969) Physical adsorption of gases. Kolloid-Zeitschrift und Zeitschrift für Polymere 235:1203–1213. https://doi.org/10.1007/BF01542530

Karimi M, Silva JAC, Gonçalves CNP, Diaz de Tuesta JL, Rodrigues AE, Gomes HT (2018) CO_2 capture in chemically and thermally modified activated carbons using breakthrough measurements: experimental and modeling study. Ind Eng Chem Res 57:11154–11166. https://doi.org/10.1021/acs.iecr.8b00953

Kumar KV, Sivanesan S (2006) Pseudo second order kinetic models for safranin onto rice husk: comparison of linear and non-linear regression analysis. Process Biochem 41:1198–1202. https://doi.org/10.1016/j.procbio.2005.11.014

Kumar KV, Porkodi K, Rocha F (2008) Isotherms and thermodynamics by linear and non-linear regression analysis for the sorption of methylene blue onto activated carbon: comparison of various error functions. J Hazard Mater 151:794–804. https://doi.org/10.1016/j.jhazmat.2007.06.056

Lagergren S (1898) Zur Theorie der Sogenannten adsorption Gelöster Stoffe (about the theory of so-called adsorption of soluble substances). Bihang A K Svenske Vet Ak Handl 24/II:1-39

Langmuir I (1918) The adsorption of gases on plane surfaces of glass, mica and platinum. J Am Chem Soc 40:1361–1403. https://doi.org/10.1021/ja02242a004

Li C, Chen L, You X (2014) Extraction of Sudan dyes from environmental water by hemimicelles-based magnetic titanium dioxide nanoparticles. Environ Sci Pollut Res Int 21:12382–12389. https://doi.org/10.1007/s11356-014-3153-8

Lopes ECN, dos Anjos FSC, Vieira EFS, Cestari AR (2003) An alternative Avrami equation to evaluate kinetic parameters of the interaction of Hg(II) with thin chitosan membranes. J Colloid Interface Sci 263:542–547. https://doi.org/10.1016/s0021-9797(03)00326-6

Low MJD (1960) Kinetics of chemisorption of gases on solids. Chem Rev 60:267–312. https://doi.org/10.1021/cr60205a003

Machín-Ramírez C, Okoh AI, Morales D, Mayolo-Deloisa K, Quintero R, Trejo-Hernández MR (2008) Slurry-phase biodegradation of weathered oily sludge waste. Chemosphere 70:737–744. https://doi.org/10.1016/j.chemosphere.2007.06.017

Maksin DD, Nastasovic AB, Milutinovic-Nikolic AD, Surucic LT, Sandic ZP, Hercigonja RV, Onjia AE (2012) Equilibrium and kinetics study on hexavalent chromium adsorption onto diethylene triamine grafted glycidyl methacrylate based copolymers. J Hazard Mater 209-210:99–110. https://doi.org/10.1016/j.jhazmat.2011.12.079

Malash GF, El-Khaiary MI (2010a) Methylene blue adsorption by the waste of Abu-Tartour phosphate rock. J Colloid Interface Sci 348:537–545. https://doi.org/10.1016/j.jcis.2010.05.005

Malash GF, El-Khaiary MI (2010b) Piecewise linear regression: a statistical method for the analysis of experimental adsorption data by the intraparticle-diffusion models. Chem Eng J 163:256–263. https://doi.org/10.1016/j.cej.2010.07.059

Malik PK (2003) Use of activated carbons prepared from sawdust and rice-husk for adsorption of acid dyes: a case study of Acid Yellow 36. Dyes Pigments 56:239–249. https://doi.org/10.1016/s0143-7208(02)00159-6

Mezenner NY, Bensmaili A (2009) Kinetics and thermodynamic study of phosphate adsorption on iron hydroxide-eggshell waste. Chem Eng J 147:87–96. https://doi.org/10.1016/j.cej.2008.06.024

Noguerol-Cal R, López-Vilariño JM, Fernández-Martínez G, Barral-Losada L, González-Rodríguez MV (2008) High-performance liquid chromatography analysis of ten dyes for control of safety of commercial articles. J Chromatogr A 1179:152–160. https://doi.org/10.1016/j.chroma.2007.11.099

Oladoja NA (2015) A critical review of the applicability of Avrami fractional kinetic equation in adsorption-based water treatment studies. Desalin Water Treat 57:15813–15825. https://doi.org/10.1080/19443994.2015.1076355

Oliveira AAS, Teixeira IF, Christofani T, Tristão JC, Guimarães IR, Moura FCC (2014) Biphasic oxidation reactions promoted by amphiphilic catalysts based on red mud residue. Appl Catal B 144:144–151. https://doi.org/10.1016/j.apcatb.2013.07.015

Podder MS, Majumder CB (2016) Kinetic, mechanistic and thermodynamic studies of removal of arsenic using Bacillus arsenicus MTCC 4380 immobilized on surface of granular activated carbon/$MnFe_2O_4$ composite. Groundwater Sustain Dev 2-3:53–72. https://doi.org/10.1016/j.gsd.2016.05.005

Qiu H, Lv L, Pan B-c, Q-j Z, W-m Z, Q-x Z (2009) Critical review in adsorption kinetic models. J Zhejiang Unive-Sc A 10:716–724. https://doi.org/10.1631/jzus.A0820524

Quesada-Peñate I, Julcour-Lebigue C, Jáuregui-Haza U-J, Wilhelm A-M, Delmas H (2009) Comparative adsorption of levodopa from aqueous solution on different activated carbons. Chem Eng J 152:183–188. https://doi.org/10.1016/j.cej.2009.04.039

Radke CJ, Prausnitz JM (1972) Adsorption of organic solutes from dilute aqueous solution of activated carbon. Ind Eng Chem Fundam 11:445–451. https://doi.org/10.1021/i160044a003

Redlich O, Peterson DL (1959) A useful adsorption isotherm. J Phys Chem 63:1024–1024. https://doi.org/10.1021/j150576a611

Reichenberg D (1953) Properties of ion-exchange resins in relation to their structure. III. Kinetics of Exchange. J Am Chem Soc 75:589–597. https://doi.org/10.1021/ja01099a022

Ribeiro RS, Silva AMT, Figueiredo JL, Faria JL, Gomes HT (2013) The influence of structure and surface chemistry of carbon materials on the decomposition of hydrogen peroxide. Carbon 62:97–108. https://doi.org/10.1016/j.carbon.2013.06.001

Rincón-Silva NG, Moreno-Piraján JC, Giraldo L (2015) Equilibrium, kinetics and thermodynamics study of phenols adsorption onto activated carbon obtained from lignocellulosic material (Eucalyptus globulus labill seed). Adsorpt 22:33–48. https://doi.org/10.1007/s10450-015-9724-2

Rodriguez A, Garcia J, Ovejero G, Mestanza M (2009) Adsorption of anionic and cationic dyes on activated carbon from aqueous solutions: equilibrium and kinetics. J Hazard Mater 172:1311–1320. https://doi.org/10.1016/j.jhazmat.2009.07.138

Saadi R, Saadi Z, Fazaeli R, Fard NE (2015) Monolayer and multilayer adsorption isotherm models for sorption from aqueous media. Korean J Chem Eng 32:787–799. https://doi.org/10.1007/s11814-015-0053-7

Savić JZ, Vasić VM (2006) Thermodynamics and kinetics of 1,8-dihydroxy-2-(imidazol-5-ylazo)-naphthalene-3,6-disulphonic acid immobilization on Dowex resin. Colloids Surf A Physicochem Eng Asp 278:197–203. https://doi.org/10.1016/j.colsurfa.2005.12.025

Secula MS, Cagnon B, Crețescu I, Diaconu M, Petrescu S (2011) Removal of an acid dye from aqueous solutions by adsorption on a commercial granular activated carbon: equilibrium, kinetic and thermodynamic study. St Cerc St CICBIA 12:307–322

Sun X, Ou H, Miao C, Chen L (2015) Removal of Sudan dyes from aqueous solution by magnetic carbon nanotubes: equilibrium, kinetic and thermodynamic studies. J Ind Eng Chem 22:373–377. https://doi.org/10.1016/j.jiec.2014.07.034

Teixeira RNP, Neto VOS, Oliveira JT, Oliveira TC, Melo DQ, Silva MAA, Nascimento RF (2013) Study on the use of roasted barley powder for adsorption of Cu^{2+} ions in batch experiments and in fixed-bed columns. Bioresources 8:3556–3573

Tosun I (2012) Ammonium removal from aqueous solutions by clinoptilolite: determination of isotherm and thermodynamic parameters and comparison of kinetics by the double exponential model and conventional kinetic models. Int J Environ Res Public Health 9:970–984. https://doi.org/10.3390/ijerph9030970

Tóth J (1981) A uniform interpretation of gas/solid adsorption. J Colloid Interface Sci 79:85–95. https://doi.org/10.1016/0021-9797(81)90050-3

Vargas AMM, Cazetta AL, Kunita MH, Silva TL, Almeida VC (2011) Adsorption of methylene blue on activated carbon produced from flamboyant pods (Delonix regia): study of adsorption isotherms and kinetic models. Chem Eng J 168:722–730. https://doi.org/10.1016/j.cej.2011.01.067

Wang L (2012) Application of activated carbon derived from ‘waste’ bamboo culms for the adsorption of azo disperse dye: kinetic, equilibrium and thermodynamic studies. J Environ Manag 102:79–87. https://doi.org/10.1016/j.jenvman.2012.02.019

Weber WJ, Morris JC (1963) Kinetics of adsorption on carbon from solution. J Sanit Eng Div 89:31–60

Yu L, Han M, He F (2017) A review of treating oily wastewater. Arab J Chem 10:S1913–S1922. https://doi.org/10.1016/j.arabjc.2013.07.020

Zhang Z, Zhang H, Hu Y, Yao S (2010) Synthesis and application of multi-walled carbon nanotubes-molecularly imprinted sol-gel composite material for on-line solid-phase extraction and high-performance liquid chromatography determination of trace Sudan IV. Anal Chim Acta 661:173–180. https://doi.org/10.1016/j.aca.2009.12.024